On direct-writing methods for electrically contacting GaAs and Ge nanowire devices

Guannan Chen, Eric M. Gallo, Joan Burger, Bahram Nabet, Adriano Cola, Paola Prete, Nico Lovergine, and Jonathan E. Spanier'

Citation: Appl. Phys. Lett. **96**, 223107 (2010); doi: 10.1063/1.3441404
View online: http://dx.doi.org/10.1063/1.3441404
View Table of Contents: http://aip.scitation.org/toc/apl/96/22
Published by the American Institute of Physics

On direct-writing methods for electrically contacting GaAs and Ge nanowire devices

Guannan Chen,[1] Eric M. Gallo,[2] Joan Burger,[1] Bahram Nabet,[2] Adriano Cola,[3] Paola Prete,[3] Nico Lovergine,[4] and Jonathan E. Spanier[1,a)]
[1]*Department of Materials Science and Engineering, Drexel University, Philadelphia, Pennsylvania 19104, USA*
[2]*Department of Electrical and Computer Engineering, Drexel University, Philadelphia, Pennsylvania 19104, USA*
[3]*Istituto per la Microelettronica e Microsistemi (IMM), Consiglio Nazionale delle Richerche (CNR), Lecce 73100, Italy*
[4]*Department of Innovation Engineering, Universitá del Salento, Lecce 73100, Italy*

(Received 5 April 2010; accepted 9 May 2010; published online 2 June 2010)

The electronic transport and gating characteristics in GaAs and Ge nanowires (NWs) are altered significantly following either indirect or direct exposure to a focused Ga^+ ion beam (FIB), such as that used to produce Pt electrical contacts to NWs. While these results challenge the assumptions made in some previously reported work relating to the electronic properties of semiconductor NWs using FIB-assisted production of contacts and/or their leads, local electron beam induced deposition is shown to be a reliable and facile route for producing robust electrical contacts to individual vapor phase-grown NWs in a manner that enables study of their actual carrier transport properties. © *2010 American Institute of Physics*. [doi:10.1063/1.3441404]

Semiconductor nanowires (NWs) continue to attract significant interest due to their potential as elements in high-performance electronic and optoelectronic devices.[1–3] Rapid evaluation of their electronic transport properties is essential to quantifying dopant composition, to achieving growth process control, and to the rapid prototyping of latest devices. A single-step method capable of electrically interfacing NWs with contacts that are stable under thermal and voltage cycling, and with precise control of their placement, can aid significantly in developing reliable NW-based devices. In recent years, local deposition of metal contacts on Si,[4] Ge,[5] SiGe,[6] GaAs,[7] GaN,[8] ZnO,[9] and chalcogenide[10] NWs using a focused Ga^+ ion beam (FIB) has emerged as an attractive alternative to multi-step processes involving electron-beam or photolithographic patterning of a resist followed by physical vapor-deposited metal and lift-off. Despite numerous reports of application of FIB to contacting individual NWs and their subsequent analyses, remarkably little is known about the effects of FIB exposures,[11] both direct and proximally indirect, on the electronic transport properties of semiconductor NWs. Here, we quantify the effects of focused Ga^+ beam exposures on sets of GaAs and Ge NWs that have been contacted using several different methods as follows: electron beam lithography (EBL), electron beam induced deposition (EBID) of Pt, and ion beam induced deposition (IBID) of Pt. FIB treatments, including exposures introduced at some distance from each NW, are seen to modify significantly the response of the NW to electrostatic gating.

GaAs and Ge NW materials, grown without intentional doping, were chosen for this study to provide two examples of the impact of ion beam processing in the contacting of NWs. Ge NWs were chosen since their transport properties are well-characterized.[12–15] In contrast, there have been no reports published on the transport properties of vapor-phase grown and not intentionally doped GaAs NWs exhibiting Ohmic contact behavior obtained without the use of a FIB. Here, GaAs NWs were grown using colloidal Au-nanoparticle-catalyzed metal-organic vapor phase epitaxy on (111)B-terminated GaAs substrates using $(CH_3)_3Ga$ and $(C_4H_9)AsH_2$ and at a growth temperature of 400 °C.[16] Ge NWs were grown using Au film-catalyzed chemical vapor deposition with GeH_4 in H_2 gas. The growth procedure involved a 10 min H_2 preannealing at 330 °C, followed by flowing the precursor and carrier gases at 300 °C for 10 min. The lengths of GaAs and Ge NWs vary in the 4–6 μm interval; diameters of the GaAs and Ge NWs were between 70–100 nm and 40–90 nm, respectively. Following sonication in isopropyl alcohol to remove the NWs from their growth substrates, NWs in solution were then transferred onto *p*-type Si(100) substrates, each possessing a 200-nm-thick thermally-grown SiO_2 gate oxide. Ti/Au bilayers (10 nm/150 nm) were previously deposited by electron-beam evaporation, and patterned into contact pads using EBL.

Contacts to GaAs and to Ge NWs were each produced using the following methods: (i) EBID of Pt; (ii) IBID of Pt, and (iii) EBL patterning of metal deposited via electron beam evaporation. While the EBID process is nondestructive, the composition and electrical properties of EBID-produced Pt are known to evolve with thickness,[17] resulting in a change from thermally activated to metallic conduction. Here, a 500-nm-thick, 250-nm-wide EBID-produced Pt lead (5 kV and 56 pA) exhibited a resistivity of (8.3×10^{-3} Ω cm) at both 80 and 400 K (not shown). EBID was then used to deposit 500-nm-thick Pt contacts onto 10 GaAs NWs and onto 5 Ge NWs, and to connect the leads to Ti/Au contact pads by employing $(CH_3)Pt(CpCH_3)$. For comparison, IBID of Pt (30 kV and 30 pA) was also carried out on a separate set of GaAs and Ge NWs. Separately, EBL patterning of metal film deposited via evaporation (electron-beam deposition of Pd/Ge/Pd trilayers, 10 nm/40 nm/10 nm) was used to

a)Electronic mail: spanier@drexel.edu.

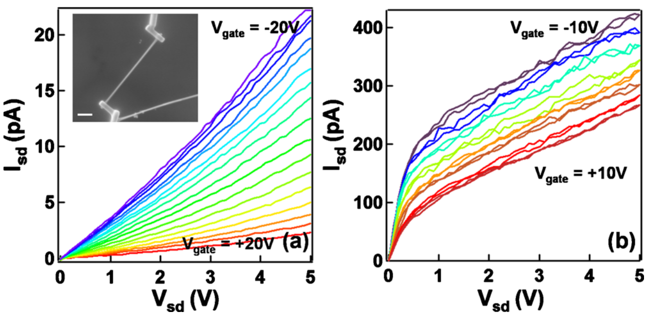

FIG. 1. (Color online) Measured source-drain I-V traces on (a) an EBL-contacted GaAs NW for $-20\ \text{V}<V_g<20\ \text{V}$ (2.5 V increment) and (b) an EBID-contacted Ge NW ($-10\ \text{V}<V_g<10\ \text{V}$, 3 V increment). The inset in (a) is an SEM top-view (scale=1 μm) of the EBID contacts on the GaAs NW.

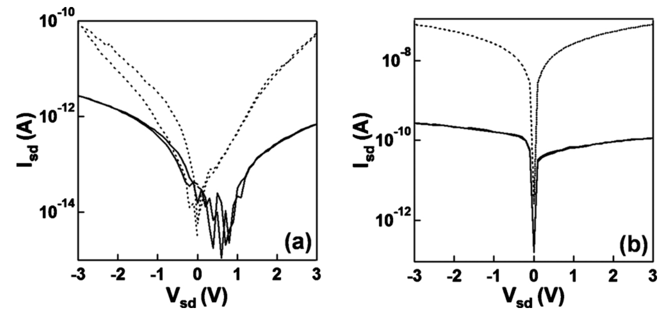

FIG. 2. I-V traces before (solid) and after (dashed) ion beam irradiation of EBID-contacted (a) GaAs and (b) Ge NWs.

contact other subsets of GaAs NWs. An optimization of the film thickness, composition and a rapid thermal anneal (400 °C, 30 s) was performed to obtain Ohmic contact to the GaAs NWs. In addition, identical sets of both IBID and EBID contacts were also prepared, without NWs, to validate that the measured currents were not due to a possible leakage current path.

The electronic transport properties of the EBL and EBID-contacted GaAs and Ge NW devices were collected under vacuum ($<10^{-5}$ torr), at selected temperatures between 80 and 400 K, and under a range of combinations of source-drain and gate biases enabled by a Ti–Au film on the back of each substrate. Response to optical illumination was facilitated by an unfocused 150 W halogen lamp placed 5 cm from the NWs. Three-terminal measurements were carried out on EBL-contacted GaAs and Ge NWs using substrate gating (±10, ±20, and ±50 V) and source-drain bias ($-5\ \text{V}<V_{sd}<+5\ \text{V}$) in order to ascertain the doping type of the as-grown NWs, not previously reported in GaAs NWs grown from the vapor phase without intentional doping. Representative I-V data plotted at selected gate voltages for the as-EBL-contacted GaAs and Ge NWs [Figs. 1(a) and 1(b), respectively] demonstrate gating in each NW type, with *p*-type character. Representative I-V traces from EBID-contacted GaAs NWs exhibit a light/dark ratio of ~1.5–5 (not shown). After the initial transport measurements the NW devices were transferred immediately into a FIB (FEI Strata 235) for the ion-beam exposures. The electron beam and ion beam (30 kV and 10–15 pA) were well-aligned in order to precisely locate the ion beam. The final setting enabled the incident ion-beam irradiation to be confined within the NW area, resulting in a typical ion beam dose on the order of $2.2\times10^{15}\ \text{cm}^{-2}$ on each NW. An identical series of electrical transport measurements were performed on the EBL- and EBID-contacted GaAs and Ge NWs following their exposures to the ion beam.

Shown in Figs. 2(a) and 2(b) are representative I-V traces of an EBID-contacted Ge NW and an EBID-contacted GaAs NW prior to (solid line) the ion beam exposure, respectively. These data were similar to those collected from the other EBID-contacted GaAs and Ge NWs, where the currents in each were in the picoampere and nanoampere ranges, respectively. For Ge NWs of this diameter range, this I-V characteristic and current at 3 V are consistent with previous reports on Ge NWs grown without intentional doping and contacted using Ti/W.[12] The dashed lines in Figs. 2(a) and 2(b) correspond to the I-V traces for the same EBID-contacted GaAs and Ge NWs following ion beam exposure as described above. In all NWs studied the current measured following ion beam exposure was seen to increase by two to three orders of magnitude, and the light response (in the GaAs NW) and variation with gating (in both GaAs and Ge NWs) could no longer be discerned.

The measured transport in the Pt-contacted NWs can be described in terms of an MSM structure.[18] The current increase by two to three orders of magnitude after ion-beam irradiation on NWs is consistent with a relatively high-dose ion beam implantation. We calculated the 30 kV Ga^+ ion stopping range by a transport range of ions in matter (TRIM) simulation.[19] The results showed that the ion traveling distance peaked at 18.3 nm and 18.2 nm in GaAs and Ge, respectively, and an appreciable concentration of ions extends 50 nm under the surface. Considering that the NWs have a diameter range between 40 and 100 nm, the implantation can be expected to reach well within each NW. As observed in bulk GaAs, the Ga^+ beam implantation can be expected to generate electrically active defects, creating acceptor states and resulting in an increase in carrier concentration in *p*-type GaAs as a function of Ga^+ dose.[20] Thus, the increase in current indicates that the acceptor states, through implantation in the *p*-type NWs, causing the Fermi level to move closer to the valence band. Changes in both NW conductivity and metal-semiconductor contact properties[21] can be responsible for the observed substantial increase in conduction. The lack of light response in postprocessed NWs is also expected as the number of optically generated carriers is negligible compared to dark conditions. Further, high doping of the NWs can be expected to reduce the gating effect, consistent with the data.

GaAs and Ge NWs, contacted using Pt via IBID, were reported to have exhibited a linear current-voltage response,[7,11] indicative of Ohmic contacts. The Pt work function and electron affinity of GaAs suggest that deposited Pt, even with annealing, cannot account for the observed responses. A focused 30 keV ion-beam has a dropletlike-shaped interaction volume ($\sim6.5\times10^4\ \text{nm}^3$) that is much larger than that for a typical NW, and the implanted Ga^+ are expected to have a lateral Gaussian distribution >500 nm from the beam spot.[20] Besides Ga^+ ion implantation, the electronic transport in long (>1 μm) NWs is also influenced by IBID lateral proximity effects. To demonstrate the spatial proximity extent of ion beam exposure, the NW devices were also placed in the scanning electron microscope (SEM)-FIB while the ion beam (30 kV/30 pA) was incident on the substrate for IBID of a Pt patch over an area of

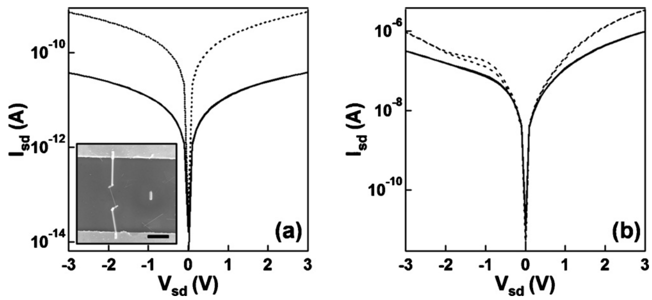

FIG. 3. I-V traces for (a) GaAs and (b) Ge NWs collected before (solid) and after (dashed) an IBID Pt patch was deposited 10 μm from each NW. Inset: SEM image of the IBID Pt patch in relation to the GaAs NW. (scale: 5 μm).

1.5 μm^2/dose of 3×10^{17} cm^{-2} at 10 μm from the NW [inset of Fig. 3(a)]. The currents were seen to increase by one to two orders of magnitude, even when the ion beam exposure was limited to some distance from the NW device [Figs. 3(a) and 3(b)].[22] This effect may be attributed to the surface deposition of recoiled Ga^+ ions that readily oxidize under the relatively low vacuum environment of the FIB, suggesting that connecting EBID contacts to probe and/or bonding contact pads with IBID lines would also change the NW transport properties.

In our comparison experiments, the transport measurements on IBID contacted GaAs NW devices produced with 30 pA/30 kV exhibited a linear I-V response and a resistance of 3.75×10^7 Ω (80 nA at 3 V). However, the transport experiments from EBL-contacted GaAs NWs taken from the same batch also exhibited Ohmic contacts but showed that these GaAs NWs in fact have a resistivity four orders of magnitude higher. This enormous difference, taken with other reports on the implantation of Ga^+ and amorphization[11] demonstrate that IBID of Pt significantly modifies the NW transport properties.

Low-current 30 kV FIB irradiation on or near semiconductor NWs is seen to alter their carrier transport. Orders of magnitude increases in current are accompanied by diminished photocurrent and gating responses. For direct ion beam exposure, these results can be ascribed primarily to Ga^+ implantation in the NWs, resulting in the additional doping of GaAs NWs which can also alter contact properties. For indirect exposure the results can be attributed to the recoiling of Ga^+ ions that readily oxide under the relatively low vacuum environment of the FIB. Thus, EBID of Pt, rather than IBID, produces contacts to semiconductor NWs in a manner that permits study of their as-grown transport properties.

The authors acknowledge the Central Research Facility at Drexel University and the assistance of Craig L. Johnson and Ed Gasgall in using the SEM-FIB in this work. This work was supported by the NSF under Grant Nos. DMR-0907381, DMR-0722845, and ECCS-0702716, by the ARO under Grant No. W911NF-08-1-0067, and with additional support from Air Products Corporation.

[1] A. Javey, S. Nam, R. S. Friedman, H. Yan, and C. M. Lieber, Nano Lett. **7**, 773 (2007).
[2] Y. Gu, E. S. Kwak, J. L. Lensch, J. E. Allen, T. W. Odom, and L. J. Lauhon, Appl. Phys. Lett. **87**, 043111 (2005).
[3] B. Z. Tian, X. L. Zheng, Y. Fang, N. Yu, G. Yu, J. Huang, T. J. Kempa, and C. M. Lieber, Nature (London) **449**, 885 (2007).
[4] A. I. Hochbaum, R. Chen, R. D. Delgado, W. Liang, E. C. Garnett, M. Najarian, A. Majumdar, and P. D. Yang, Nature (London) **451**, 163 (2008).
[5] T. Hanrath and B. A. Korgel, J. Phys. Chem. B **109**, 5518 (2005).
[6] C. Qi, Y. Rangineni, G. Goncher, R. Solkani, K. Langworthy, and J. Jordan, J. Nanosci. Nanotechnol. **8**, 457 (2008).
[7] S. Thunich, L. Prechtel, D. Spirkoska, G. Abstreiter, A. Fontcuberta i Morral, and A. W. Holleitner, Appl. Phys. Lett. **95**, 083111 (2009).
[8] C. Y. Nam, J. Y. Kim, and J. E. Fischer, Appl. Phys. Lett. **86**, 193112 (2005).
[9] Y. Ma, Z. Zhang, L. Lu, A. Jin, and C. Gu, Nanotechnology **16**, 746 (2005).
[10] Y. Jung, C. Yang, S. Lee, and R. Agarwal, Nano Lett. **9**, 2103 (2009).
[11] T. Hanrath and B. A. Korgel, *Proceedings of the Institution of Mechanical Engineers, Part N: Journal of Nanoengineering and Nanosystems* (Professional Engineering Publishing, Westminster, London, 2004), Vol. 218, p. 25.
[12] D. Wang, Q. Wang, A. Javey, R. Tu, H. Dai, H. Kim, R. B. Wehrspohn, P. C. McIntyre, T. Krishnamohan, and K. C. Saraswat, Appl. Phys. Lett. **83**, 2432 (2003).
[13] S. Zhang, E. R. Hemesath, D. E. Perea, E. Wijaya, J. L. Lensch-Falk, and L. J. Lauhon, Nano Lett. **9**, 3268 (2009).
[14] W. Lu, J. Xiang, B. P. Timko, Y. Wu, and C. M. Lieber, Proc. Natl. Acad. Sci. U.S.A. **102**, 10046 (2005).
[15] B. Yu, X. H. Sun, G. A. Calebotta, G. R. Dholakia, and M. Meyyappan, J. Cluster Sci. **17**, 579 (2006).
[16] P. Paiano, P. Prete, E. Speiser, N. Lovergine, W. Richter, L. Tapfer, and A. M. Mancini, J. Cryst. Growth **298**, 620 (2007).
[17] J. M. De Teresa, R. Cordoba, A. Fernandez-Pacheco, O. Montero, P. Strichovanec, and M. R. Ibarra, J. Nanomater. **2009**, 936863(2009).
[18] S. M. Sze, D. J. Coleman, and A. Loya, Solid-State Electron. **14**, 1209 (1971).
[19] J. F. Ziegler, http://www.srim.org.
[20] S. J. Brown, P. D. Rose, G. A. C. Jones, E. H. Linfield, and D. A. Ritchie, Appl. Phys. Lett. **74**, 576 (1999).
[21] S. M. Sze and K. K. Ng, *Physics of Semiconductor Devices*, 3rd ed. (Wiley, New York, 2007).
[22] Y. K. Park, T. Nagai, M. Takai, C. Lehrer, R. Frey, and H. Ryssel, *Proceedings of the International Conference on Ion Implantation Technology*, (IEEE, New York, 1998), Vol. 2, pp. 1137.